Acta Materia Medica

Short Communication

Structure-based virtual screening for novel p38 MAPK inhibitors and a biological evaluation

Graphical abstract

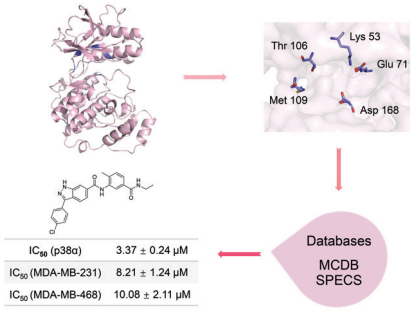

Highlights

- Compound **10** was identified as a promising inhibitor of p38α, exhibiting an IC50 value of 3.37 ± 0.24 μM.
- Compound **10** inhibited the proliferation of MDA-MB-231 and MDA-MB-468 cells effectively, with IC50 values of 8.21 ± 1.24 μM and 10.08 ± 2.11 μM, respectively.
- Compound **10** caused autophagic cell death.

Authors

Qinwen Zheng, Yumeng Zhu, Aoxue Wang, Panpan Yang, Xin Wang, Wen Shuai, Liang Ouyang and Guan Wang

Correspondence

shuaiwen05@163.com (W. Shuai); ouyangliang@scu.edu.cn (L. Ouyang); guan8079@163.com (G. Wang)

In brief

Compound **10**, obtained through a multi-step virtual screening process, is a potent p38α inhibitor. The finding contributes valuable insights into the study of p38α-related therapy and the development of targeted drugs for p38α.

https://doi.org/10.15212/AMM-2023-0028
Acta Materia Medica 2023, Volume 2, Issue 4, p. 377-385

Acta
Materia
Medica

Short Communication

Structure-based virtual screening for novel p38 MAPK inhibitors and a biological evaluation

Qinwen Zheng[a,1], Yumeng Zhu[a,1], Aoxue Wang[a,1], Panpan Yang[a], Xin Wang[a], Wen Shuai[a,*], Liang Ouyang[a,*] and Guan Wang[a,*]

[a]Department of Biotherapy, Cancer Center and State Key Laboratory of Biotherapy, Innovation Center of Nursing Research, Nursing Key Laboratory of Sichuan Province, West China Hospital, Sichuan University/West China School of Nursing, Sichuan University, Chengdu 610041, China

[1]These authors made equal contributions to this work.

***Correspondence:** shuaiwen05@163.com (W. Shuai); ouyangliang@scu.edu.cn (L. Ouyang); guan8079@163.com (G. Wang)

Received: 16 July 2023; Revised: 18 September 2023; Accepted: 4 October 2023

Published online: 26 October 2023

DOI 10.15212/AMM-2023-0028

ABSTRACT

Mitogen-activated protein kinases (MAPKs) are a group of serine-threonine protein kinases that can be activated by extracellular stimuli. MAPK14 (p38α) affects major disease processes, while inhibition of p38α has been shown to have potential therapeutic effects. Many inhibitors targeting p38α have entered clinical trials but have a long development cycle and severe side effects. We developed a multi-step receptor structure-based virtual screening method to screen potential bioactive molecules from SPECS and our MCDB libraries. Compound **10** was identified as a promising p38α inhibitor that may be used in the treatment of p38αMAPK pathway-related diseases, but corollary studies are warranted.

Keywords: p38α, inhibitors, virtual screening, activity test

1. INTRODUCTION

The p38 mitogen-activated protein kinase (MAPK) was first identified while studying the effect of a hypertonic environment on fungi. The p38 MAPK was initially thought to be a stress-activated protein kinase, like the c-Jun N-terminal kinase (JNK). In recent years, however, it has been shown that p38 MAPK has a role in a variety of tumors. There are four p38 MAPK isoforms (p38α [MAPK14], p38β [MAPK11], p38γ [MAPK12], and p38δ [MAPK13]). The distribution of the four isoforms is tissue-specific. While p38α and p38β are widely present in various tissues, p38γ is only present in skeletal muscles and p38δ is mainly present in glandular tissues.

There is a close relationship between p38 MAPK and cancer. In normal physiologic activities, p38 MAPK is related to the cell cycle, differentiation, metabolism, and senescence. Whitaker et al. [1] demonstrated that p38 affects G1 and G2 phases in the cell cycle and Weng et al. [2] confirmed that amiodarone regulates cell proliferation and myofibroblast differentiation in human embryonic lung fibroblasts (HELFs) by regulating the p38 MAPK pathway, while cancer cells can destroy the pathway to promote proliferation, survival, and invasion. The p38 MAPK pathway regulates cell cycle progression and cellular programs for cell survival and differentiation at different transition points via transcription-dependent mechanisms [3], which contributes to the impact on a variety of cancers. In many cancer cells, such as liver and lung cancers, the activation of p38α is usually associated with anti-proliferative function. Abnormal proliferation of various types of primary cells, including cardiomyocytes, hepatocytes, fibroblasts, hematopoietic cells, and lung cells, is negatively regulated by p38α [4-6]. In addition, p38α can promote apoptosis in some cells. In the early transformation process, reactive oxygen species (ROS) can induce activation of p38α to induce cell apoptosis, thereby preventing the carcinogenic effect caused by the accumulation of ROS [7]. Cell survival is also mediated by p38α through a quiescent state (cancer quiescence), which is important for cancer cell resistance. Moreover, p38α is associated with the G2/M checkpoint, which induces cell cycle arrest and promotes DNA repair, possibly leading to apoptotic resistance of cancer cells

Acta Materia Medica

[8]. Therefore, developing inhibitors targeting p38α, which is the most widely distributed and influential p38 isoform, is a priority.

Computer-aided drug design (CADD) has changed the traditional drug design industry in recent years. CADD consists of two technologies (structure-based drug design [SBDD] and ligand-based drug design [LBDD]), which have good accuracy in the field of developing drug lead molecules [9]. SBDD is recognized as an optimal method to generate and optimize ligands for the pharmaceutical industry [10]. The basic steps of SBDD are further divided into target preparation, binding site identification, molecular docking, virtual screening, and molecular dynamics. Among the steps, structure-based virtual screening (SBVS) is used to screen novel bioactive compounds against specific therapeutic targets from various compound libraries in early drug development projects. In addition to predicting binding modes, SBVS also ranks the docked molecules by docking scores. This rating can be used as the sole criterion for selecting out hits. Moreover, SBVS can be combined with other evaluation methods, such as in combination with biological assays, to determine the biological activity of hits against the molecular target under study [11].

Herein we used a SBVS approach to screen lead compounds inhibiting p38α from compound libraries we established via multiple screening processes. Among the compounds, compound **10** showed potential inhibitory activity against p38α, and is thus a promising lead compound for further investigation.

2. RESULTS AND DISCUSSION

2.1 SBVS

The most significant advantage of SBVS is efficiently identifying novel chemical structures against targets of interest from large chemical libraries. To more precisely improve the selectivity of p38α inhibitors, key residues in the p38α binding pocket were analyzed. By analyzing all co-crystal structures contained in the protein data bank (PDB), Asp168, Glu71, and Met109 were shown to be key amino acid residues in the interaction (**Figure 1**). Subsequently, multiple docking was performed using the Discovery Studio program to screen selective p38α inhibitors.

More than 200,000 Compounds were downloaded from the SPECS database (www.specs.net) and in-house, manually curated database MCDB (Mitotic Catastrophe Database: http://www.combio-lezhang.online/MCDB/compound_html/) prepared for virtual screening. First, the Lipinski rule of five was used to screen > 200,000 compounds in the MCDB library, which was established by our laboratory and the SPECS library. A total of 196,432 small-molecule compounds were obtained for the following docking-based virtual screening.

Next, these molecules were scored by docking analysis using the co-crystal structure of human p38αMAPK (PDB code: 1A9U) through the LibDock module in Discovery Studio 2020 Client version, Chengdu, China. The top 1000 molecules with scores between 121.995 and 153.925 were selected for the second screening. The CDOCKER module was further used to analyze the 1000 p38α screening results more accurately. The CDOCKER-energy score was obtained to screen out 10 molecules with scores > 17.6255 as candidates for further analysis. Finally, 10 candidate p38αMAPK inhibitors were identified by visual inspection of the selected library, including evaluation of shape complementarity, hydrogen bonds, hydrophobic contacts, binding pattern similarity, specific ligand-protein interactions, and docking scores, after taking into consideration the diversity of molecular frameworks (**Table 1**). The 10 compounds were used for the subsequent test of inhibition ability.

2.2 The p38α kinase inhibitory assays

Luminescence signals were detected using a multifunctional microplate reader and the ADP-GloTM luminescence method, which was converted into the corresponding amount of ATP consumed to judge cell activity. The IC_{50} was obtained after fitting the curve. Ten compounds were measured separately and the IC_{50}s are as follows. Among the 10 compounds, compound **10** showed the best inhibitory effect against p38α, with an IC_{50} value of 3.37 ± 0.24 μM.

2.3 Cell viability assay

Antoon et al. [12] demonstrated that RWJ67657, a p38α inhibitor, effectively inhibits the p38 pathway in MDA-MB-361 breast cancer cells and inhibits the growth of endocrine-resistant breast cancer tumors *in vitro* and *in vivo*. Our laboratory is committed to the development of inhibitors for triple-negative breast cancer in the long term. Therefore, MDA-MB-231 and MDA-MB-468, two triple-negative breast cancer (TNBC) cells, were selected for cell anti-proliferation experiments. The MTT assay was used to compare the number of surviving cells to obtain the cell inhibition rate under different concentration gradients. The IC_{50} value of each compound was calculated against two TNBC cells (**Table 2**). The results showed that compound **10** not only exhibited inhibitory activity in the kinase assay ($IC_{50} = 3.37 \pm 0.24$ μM), but also had a potent anti-proliferative effect on MDA-MB-231 and MDA-MB-468 cancer cells with IC_{50} values of 8.21 ± 1.24 μM and 10.08 ± 2.11 μM, respectively (**Figure 2**). In contrast, the other 9 compounds obtained by screening had slightly lower activity.

2.4 Cell death pathway assay

To explore the compound **10** cell death pathway, the cell survival rate was determined by co-treatment with several common inhibitors targeting different cell death pathways and compound **10**. Compound **10** was treated with the apoptosis inhibitor, Z-VAD-FMK, the necrosis inhibitor, Necro, the iron chelator, DFO, the ferroptosis

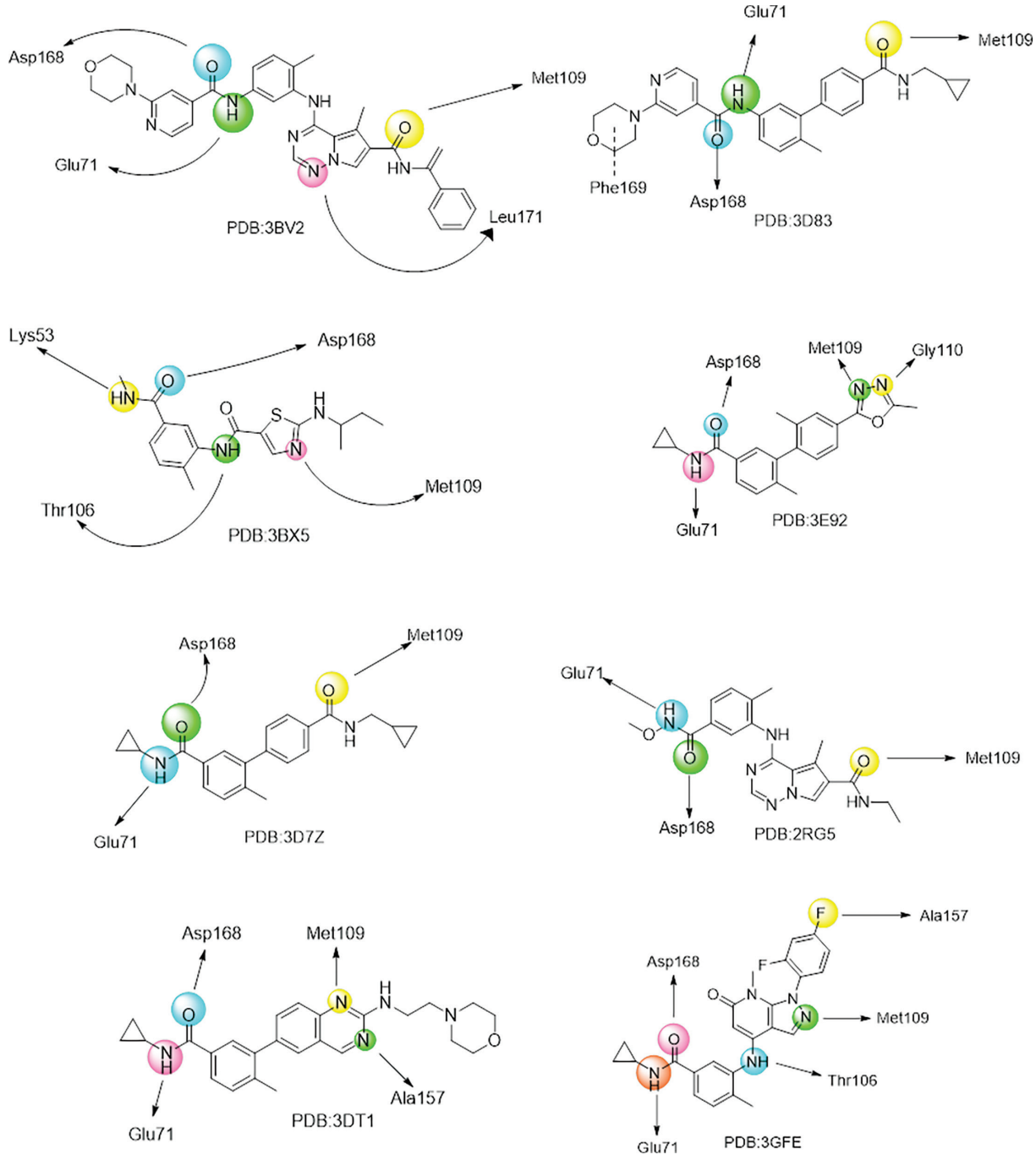

Figure 1 | The intermolecular forces and important amino acid residues of the existing inhibitors interacting with p38α.

inhibitor, Fer-1, the copper chelator, TTM, and the autophagy inhibitor, 3-MA. The maximum concentration of the corresponding inhibitors (10 μM, 30 μM, 10 μM, 125 μM, 10 μM, 10 μM, and 50 μM) was selected to have a rescue effect without killing cells more effectively. Compound **10** significantly inhibited cell viability. In the presence of 3-MA, cell viability increased from < 50% to > 80%; however, other death pathway inhibitors for rescuing cell death induced by compound **10** was almost invalid. Compound **10** indicated that autophagy inhibitor rescued the cell death induced by compound **10**, which indirectly indicated that compound **10** induced TNBC cell death through autophagy pathway (Figure 3).

Next, western blot experiments were conducted for further verification. The level of autophagy was determined by the ratio of LC3-II:I. LC3-I is formed by cleavage

Table 1 | Virtual screening results.

No.	Structure	Chemical name	–CDOCKER energy	LibDock score
1	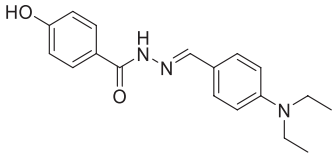	DY131	35.2763	122.036
2	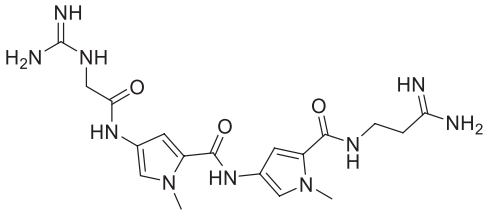	Netropsin (dihydrochloride)	52.0194	148.964
3	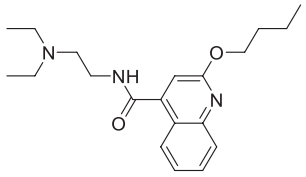	Dibucaine (hydrochloride)	17.6255	121.995
4	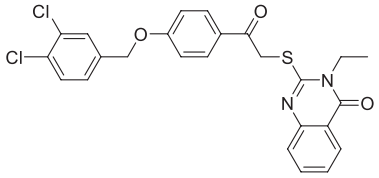	2-[(2-4-[(3,4-dichlorobenzyl)oxy] phenyl-2-oxoethyl)sulfanyl]-3-ethyl-4(3H)-quinazolinone	36.5970	153.925
5	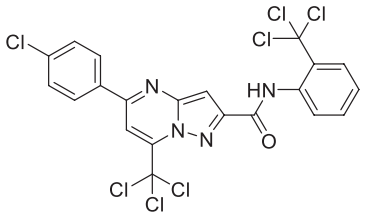	5-(4-chlorophenyl)-7-(trifluoromethyl)-N-[2-(trifluoromethyl)phenyl] pyrazolo[1,5-a]pyrimidine-2-carboxamide	29.8581	125.353
6	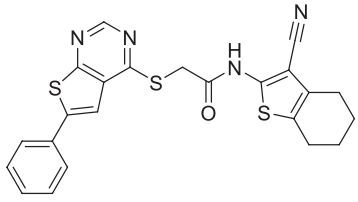	N-(3-cyano-4,5,6,7-tetrahydro-1-benzothien-2-yl)-2-[(6-phenylthieno[2,3-d]pyrimidin-4-yl) sulfanyl]acetamide	29.3654	145.929
7	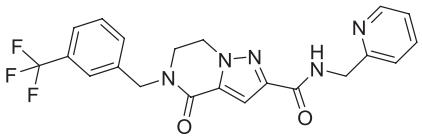	4-oxo-N-[(pyridin-2-yl)methyl]-5-[3-(trifluoromethyl)phenyl]methyl-4H,5H,6H,7H-pyrazolo[1,5-a] pyrazine-2-carb	37.0194	146.836
8	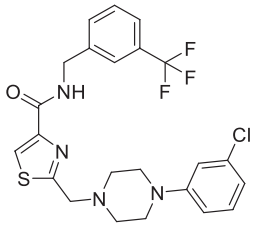	2-[4-(3-chlorophenyl)piperazin-1-yl] methyl-N-[3-(trifluoromethyl)phenyl] methyl-1,3-thiazole-4-carboxamide	40.4858	140.802

Table 1 | Continued

No.	Structure	Chemical name	–CDOCKER energy	LibDock score
9	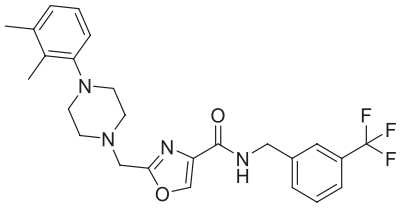	2-[4-(2,3-dimethylphenyl)piperazin-1-yl]methyl-N-[3-(trifluoromethyl) phenyl]methyl-1,3-oxazole-4-carboxamid	42.0744	142.277
10	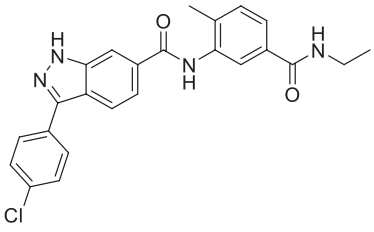	3-(4-chlorophenyl)-N-(5-(ethylcarbamoyl)-2-methylphenyl)-1H-indazole-6-carboxamide	33.8025	137.116

Table 2 | Inhibitory activities of 10 compounds against p38α, MDA-MB-231, and MDA-MB-468.

No.	Structure	p38α (IC_{50}, μM)	Anti-proliferative activity (IC_{50}, μM)	
			MDA-MB-231	MDA-MB-468
1	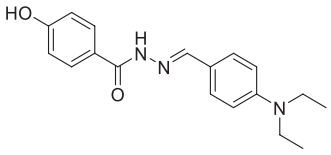	6.23 ± 1.01	19.21 ± 2.18	12.60 ± 3.02
2	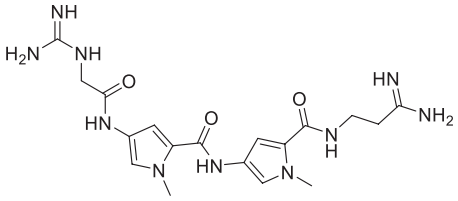	9.06 ± 3.25	15.56 ± 1.25	17.21 ± 3.88
3	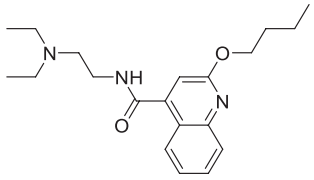	5.91 ± 0.31	9.36 ± 1.25	13.88 ± 2.08
4	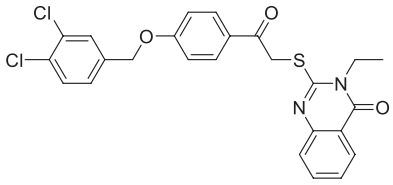	7.70 ± 1.23	9.41 ± 1.34	12.40 ± 3.96
5	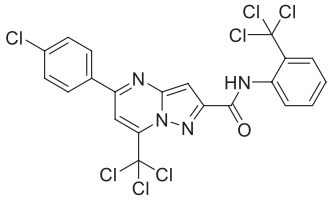	5.82 ± 0.71	15.12 ± 1.05	15.89 ± 3.11

Acta Materia Medica

Table 2 | Continued

No.	Structure	p38α (IC_{50}, μM)	Anti-proliferative activity (IC_{50}, μM)	
			MDA-MB-231	MDA-MB-468
6	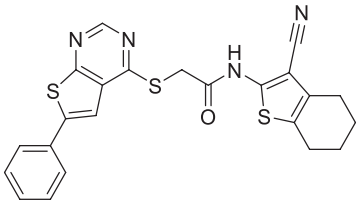	6.96 ± 0.91	20.21 ± 1.26	20.09 ± 1.09
7	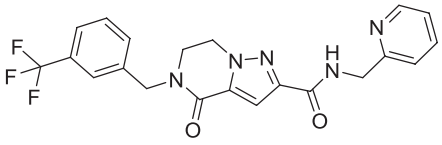	7.25 ± 2.32	15.03 ± 1.14	19.34 ± 2.05
8	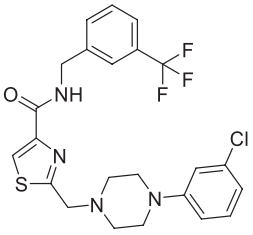	7.22 ± 1.20	18.22 ± 1.98	18.76 ± 2.03
9	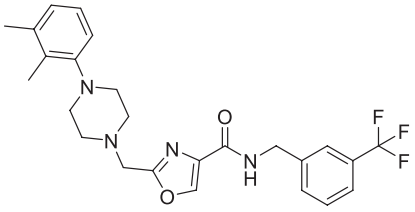	5.56 ± 1.01	11.09 ± 2.09	17.90 ± 1.90
10	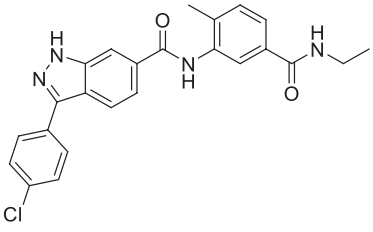	3.37 ± 0.24	8.21 ± 1.24	10.08 ± 2.11

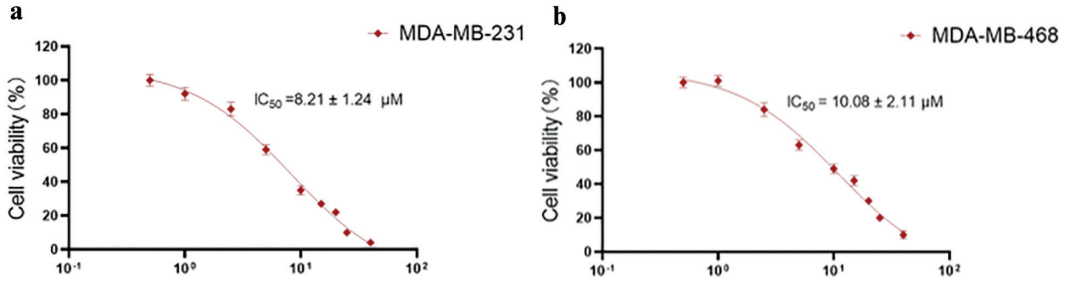

Figure 2 | (a, b) Inhibition rate-concentration curves of compound 10 on MDA-MB-231 and MDA-MB-468.

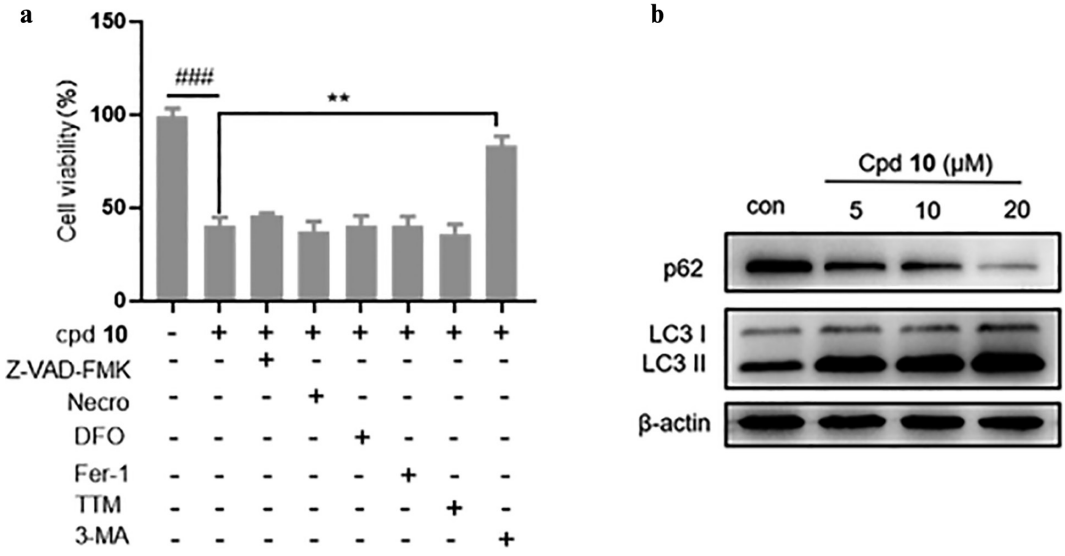

Figure 3 | (a) Co-inhibition assay of compound 10 and six other death pathway inhibitors. (b) Western blot assay of cells treated with compound 10.

of a polypeptide from the C-terminus of pro-LC3 by ATG4. When autophagy occurs, LC3-I covalently binds to phosphatidylethanolamine under the action of ATG7 and ATG12-ATG5-ATG16L to form LC3-II, which binds to the autophagosome membrane [13]. Therefore, including autophagy can lead to the transformation of LC3-I-to-LC3-II. The linker region (LRS) between the zinc finger and UBA domains of p62 protein, a widely studied autophagy substrate, is responsible for binding to the autophagy receptor, Atg8/LC3. During autophagosome formation, p62 acts as a bridge connecting LC3 to aggregated proteins and is selectively encapsulated into the autophagosome, then degraded by proteolytic enzymes in the autolysosome [14]. Therefore, the expression of p62 has a negative correlation with autophagic activity. It can be clearly seen in **Figure 3b** that compound **10** downregulated p62 and induced the conversion of LC3-I to LC3-II, indicating that compound **10** induced canonical autophagy.

Although compound **10** was successfully screened out as a p38α inhibitor with good inhibitory activity in the current study, there are still many shortcomings and further research and analysis are warranted. First, only MCDB and SPECS databases were selected for virtual screening in the current study, and the limitation of library selection restricted the screening results. Second, only one docking application, Discovery Studio, was used for virtual screening, thus the results may have differed after virtual screening using another docking application. In recent years the rapid development of artificial intelligence (AI) technology and deep learning technology has also promoted virtual screening. In the future, we can consider further understanding how tools, such as deep learning, can be used to improve the accuracy of virtual screening. Third, only two types of TNBC cells were used for the anti-proliferation assay, and the sample sizes were relatively too small. In addition, there is a problem of inhibitor selection in exploring cell death pathway experiments. Even if the selected inhibitors of the typical cell death pathway were complete, other inhibitors could be more precise as inhibitors of the same death pathway, and the selected inhibitor could interact with compound **10** resulting in reduced inhibitory activity rather than competition for the substrate. Finally, further understanding of the role of p38α *in vivo* is needed to facilitate the design of its inhibitors. In addition, the rapid development of precision medicine and biomedical technology in recent decades also provides infinite possibilities for inhibitors in the future.

In summary, p38α is one of the most important members of the MAPK family and plays an important role in a variety of diseases, such as neurodegenerative diseases, cancer, and cardiovascular diseases. Based on the structural characteristics of p38α, a multi-step structure-based virtual screening was carried out, and the most effective compound **10** was identified with an IC_{50} of 3.37 ± 0.24 μM on p38α. Compound **10** effectively inhibited the proliferation of MDA-MB-231 and MDA-MB-468 TNBC cells with IC_{50} values of 8.21 ± 1.24 μM and 10.08 ± 2.11 μM, respectively. Furthermore, we demonstrated that compound **10** caused cell death via the autophagy pathway. Western blot analysis further explored the autophagy pathway, and the results showed that compound **10** downregulated the marker substrate, p62, of autophagy and converted LC3-I to LC3-II. Our study provides more reference for research involving p38α-related therapy and the development of novel drugs targeting p38α.

ACKNOWLEDGEMENTS

This work was supported by grants from the National Natural Science Foundation of China (Grant 22177083), the Sichuan Science and Technology Program (Grant 2022NSFSC1290), the 1·3·5 Project for Disciplines of Excellence–Clinical Research Incubation Project of West China Hospital [Sichuan University] (ZYJC21016), and the West China Nursing Discipline Development Special Fund Project of Sichuan University (Grant HXHL21011).

CONFLICT OF INTEREST

No conflicts of interest.

REFERENCES

[1] Whitaker RH, Cook JG: Stress Relief Techniques: p38 MAPK Determines the Balance of Cell Cycle and Apoptosis Pathways. *Biomolecules* 2021, 11:1444.

[2] Weng J, Tu M, Wang P, Zhou X, Wang C, Wan X, et al.: Amiodarone Induces Cell Proliferation and Myofibroblast Differentiation via ERK1/2 and p38 MAPK Signaling in Fibroblasts. *Biomedicine and Pharmacotherapy* 2019, 115:108889.

[3] Wagner EF, Nebreda AR: Signal Integration by JNK and p38 MAPK Pathways in Cancer Development. *Nature Reviews Cancer* 2009, 9:537–549.

[4] Engel FB, Schebesta M, Duong MT, Lu G, Ren S, Madwed JB, et al.: p38 MAP Kinase Inhibition Enables Proliferation of Adult Mammalian Cardiomyocytes. *Genes and Development* 2005, 19:1175–1187.

[5] Hui L, Bakiri L, Mairhorfer A, Schweifer N, Haslinger C, Kenner L, et al.: p38alpha Suppresses Normal and Cancer Cell Proliferation by Antagonizing the JNK-c-Jun Pathway. *Nature Genetics* 2007, 39:741–749.

[6] Ventura JJ, Tenbaum S, Perdiguero E, Huth M, Guerra C, Barbacid M, et al.: p38alpha MAP Kinase is Essential in Lung Stem and Progenitor Cell Proliferation and Differentiation. *Nature Genetics* 2007, 39:750–758.

[7] Dolado I, Swat A, Ajenjo N, De Vita G, Cuadrado A, Nebreda AR: p38alpha MAP Kinase as a Sensor of Reactive Oxygen Species in Tumorigenesis. *Cancer Cell* 2007, 11:191–205.

[8] Thornton TM, Rincon M: Non-Classical p38 Map Kinase Functions: Cell Cycle Checkpoints and Survival. *International Journal of Molecular Sciences* 2015, 5:44–51.

[9] Batool M, Ahmad B, Choi S: A Structure-Based Drug Discovery Paradigm. *International Journal of Molecular Sciences* 2019, 20:2783.

[10] Park H, Chien PN, Ryu SE: Discovery of Potent Inhibitors of Receptor Protein Tyrosine Phosphatase Sigma through the Structure-Based Virtual Screening. *Bioorganic and Medicinal Chemistry Letters* 2012, 22:6333–6337.

[11] Gangwal RP, Damre MV, Das NR, Dhoke GV, Bhadauriya A, Varikoti RA, et al.: Structure Based Virtual Screening to Identify Selective Phosphodiesterase 4B Inhibitors. *Journal of Molecular Graphics and Modelling* 2015, 57:89–98.

[12] Antoon JW, Bratton MR, Guillot LM, Wadsworth S, Salvo VA, Elliott S, et al.: Pharmacology and Anti-Tumor Activity of RWJ67657, a Novel Inhibitor of p38 Mitogen Activated Protein Kinase. *American Journal of Cancer Research* 2012, 2:446–458.

[13] Zhang J, Wang G, Zhou Y, Chen Y, Ouyang L, Liu B: Mechanisms of Autophagy and Relevant Small-Molecule Compounds for Targeted Cancer Therapy. *Cellular and Molecular Life Sciences* 2018, 75:1803–1826.

[14] Bu F, Zhang J, Shuai W, Liu J, Sun Q, Ouyang L: Repurposing Drugs in Autophagy for the Treatment of Cancer: From Bench to Bedside. *Drug Discovery Today* 2022, 27:1815–1831.